Chapter 26
Multi-Approach Global Stability Assessment of Soil Nail Walls

Vikas Pratap Singh ⓘ

Introduction

Soil nailing is an in-situ earth retaining technique in which construction proceeds from the top to bottom by installing closely spaced passive inclusions/reinforcement in the form of steel bars (i.e., nails or tendons). These steel bars may or may not be encased in grout cover. Soil nail walls are most suitable to support in-situ excavation/slope faces that bears an inclination close to 90° (i.e., almost vertical face) with respect to the horizontal particularly encountered in applications such as approaches to the underpass and basement for multistoried buildings [1–3].

For the given in-situ soil and geometric conditions, the conventional design of soil nail walls is based on assuming a configuration of design parameters including nail spacing in horizontal and vertical directions, diameter, length and inclination of nails, etc. such that it satisfies the safety criteria against various failure modes. According to FHWA [4], the broad categories of various modes of failure for a typical soil nail wall are external failure modes (e.g., global stability, sliding stability, basal heave), internal failure modes (e.g., nail pullout failure, nail tensile failure) and facing failure modes (e.g., facing punching shear failure, facing flexure failure). Among various failure modes of soil nail walls, global stability is one of the prominent failure modes representing the overall stability of the reinforced soil mass. Global stability analysis plays a significant role in the long-term stability and overall performance of the soil nail wall.

Further, a soil nail wall is typically a three-dimensional problem of a composite material including components such as in-situ soil, steel bars (i.e., nails), and facing elements (i.e., cast in-situ concrete or pre-cast panels). Thus, global stability of soil nail walls is a function of the complex soil–structure interaction among these

V. P. Singh (✉)

National Institute of Technology Uttarakhand, Srinagar, Garhwal, Uttarakhand 246174, India
e-mail: vpsingh@nituk.ac.in

components. Also, it largely depends on the in-situ soil parameters such as cohesion c, angle of internal friction φ, and unit weight γ. In conventional design, typically a representative value of these soil parameters is adopted which fails to account for the uncertainties involved in the determination of soil parameters though field and/or laboratory experiments [5, 6].

Another important aspect in the design of soil nail walls is the consideration of the seismic loading. It has been reported in the literature that soil nail walls have performed relatively better to the other conventional gravity earth retaining structures under seismic loading [7–13]. Global stability analysis of soil nail walls subjected to the seismicity could be performed using pseudo-static limit equilibrium method [14] and/or by simulating time-history data with the help of a suitable computational tool. In the available literature, limited studies exist on the detailed analysis of the performance and stability of soil nail walls subjected to the seismic loading, and therefore, deserves further investigation.

In the present study, a typical soil nail wall of 8 m height is considered, and specifically global stability of the wall is studied under the following conditions: (a) static loading, (b) seismic loading, and (c) uncertainty in the determination of the in-situ soil parameters based on reliability concept. Study is conducted using the allowable stress design approach [4], performing numerical simulations using a two-dimensional finite element-based computational tool [15], and by Hasofer-Lind reliability method [16] for reliability analysis.

Deterministic Global Stability Analysis

As stated earlier, for deterministic global stability analysis of soil nail wall, limit equilibrium-based methodology is adopted. A planar failure surface leading to a triangular failure wedge is considered for studying the global stability under static and seismic conditions [4, 17]. Inclination of the failure surface is assumed at an angle $\psi = 45 + (\varphi/2)$ (in degrees) with respect to horizontal. Table 26.1 summarizes the design parameters and the geometric configuration of the soil nail wall considered in the study, and Fig. 26.1 shows its schematic layout along with the various forces required in the computation of the global stability.

The global stability is expressed in terms of the factor of safety FS_G which can be determined using Eqs. (26.1) and (26.2) obtained by considering the equilibrium of the resisting forces ΣR and driving forces ΣD acting tangentially to the potential failure plane.

$$FS_G = \frac{\sum R}{\sum D} \tag{26.1}$$

$$FS_G = \frac{cL_F + T_{eq}\cos(\psi - i) + \left[(W + Q_T - F_v)\cos\psi + T_{eq}\sin(\psi - i) - F_h\sin\psi\right]\tan\varphi}{(W + Q_T - F_v)\sin\psi + F_h\cos\psi} \tag{26.2}$$

Table 26.1 Details of the soil nail wall design parameters and geometric configuration

| Parameter	Value
Vertical height of wall H (m)	8.0
Nailing type	grouted
Surcharge load q_s (kPa)	0.0
Diameter of reinforcing element, i.e., nail tendon d (mm)	16.0
Drill hole diameter D_{DH} (mm)	100.0
Length of nail L (m)	4.7
Nail inclination with respect to horizontal i (degrees)	15.0
Horizontal nail spacing S_h (mm)	1.0
Vertical nail spacing S_v (mm)	1.0
Modulus of elasticity of soil, E_s, MPa	20.0
Poisson's ratio of soil, μ	0.35
Yield strength of nail, f_y, MPa	415
Modulus of elasticity of nail, E_n, GPa	200.0
Allowable bond strength, q_a (kPa)	50.0
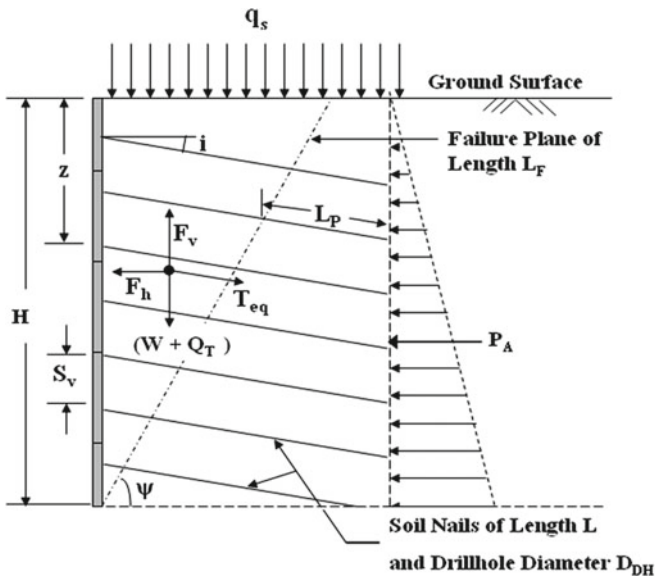
Fig. 26.1   A Schematic layout of a typical soil nail wall

where L_F (m) = length of the failure plane equal to (= $H/\sin\psi$); W (kN/m) = weight of failure wedge (= $0.5\gamma H^2 \cot\psi$); Q_T (kN/m) = total surcharge load (= $q_s H \cot\psi$); q_s (kPa) = distributed surcharge loading; T_{eq} (kN/m) = equivalent nail force [4, 18], and F_h and F_v (kN/m) = horizontal and vertical inertia forces due seismic loading considered in the pseudo-static approach, respectively, and can computed using Eqs. (26.3a, 26.3b).

$$F_h = k_h(W + Q_T) \tag{26.3a}$$

$$F_v = k_v(W + Q_T) \tag{26.3b}$$

It is to be noted that the seismic inertial forces F_h and F_v should be directed such that the resultant seismic force shall cause critical loading condition for global stability, and therefore, as shown in Fig. 26.1, the direction of the horizontal inertia force F_h is taken away from the slope and the vertical inertia force F_v is considered acting vertically upwards [4]. In the present study the earthquake data from Bhuj earthquake [19] dated January 26th, 2001 recorded at Ahmedabad station is used. Figure 26.2 shows the time-history plot of the horizontal acceleration component of the said earthquake, which is also used for the dynamic analyses using a computational tool in the subsequent sections. From the time-history plot, horizontal seismic coefficient k_h is determined equal to 0.106, and is used to compute the horizontal inertia force for the pseudo-static analysis. The vertical seismic coefficient k_v is disregarded in the present study as it results in the conservatism in the computation of global stability by reducing the self-weight component vis-à-vis shear strength along failure plane. According to FHWA [4], the typical factor of safety for global stability for soil nail walls is in between 1.35 and 1.50 for static conditions and 1.10 under seismic conditions.
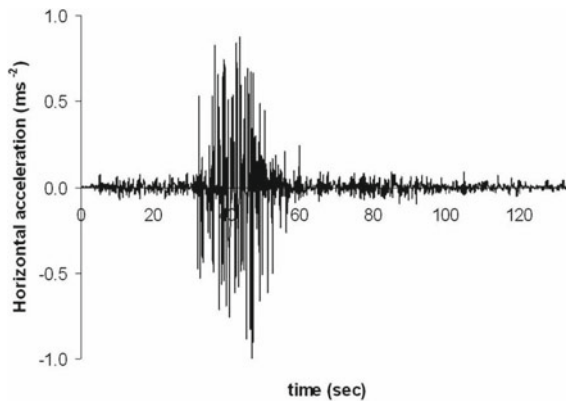

Fig. 26.2 Time-history data for Bhuj earthquake [19]

Reliability-Based Global Stability Analysis

Hasofer-Lind reliability indices [16] are determined for the global stability failure mode of the soil nail wall considered in the present study. Built-in optimization program Solver available in Microsoft Excel Program [20, 21] is used to perform the reliability analysis.

The Hasofer-Lind reliability index β can be represented in the matrix form as given by Eq. (26.4).

$$\beta = \min_{x \in F} \sqrt{\left[\frac{x_i - \mu_i^N}{\sigma_i^N}\right]^T [R]^{-1} \left[\frac{x_i - \mu_i^N}{\sigma_i^N}\right]} \tag{26.4}$$

where x_i, μ_i^N, R, and σ_i^N represent vectors/matrices of random variables, equivalent normal mean values, correlation among random variables, and equivalent normal standard deviation, respectively. F corresponds to the failure domain. For reliability analysis, three non-correlated random variables are considered, namely, in-situ soil unit weight γ and shear strength parameters (i.e., cohesion c and angle of internal friction φ). The random variables are assumed to follow the lognormal probability distribution function. Table 26.2 summarizes the statistical properties of the variables.

The limit state function (or performance function) for the global stability, *perfn(1)*, of soil nail wall is given by Eq. (26.5). Various terms in Eq. (26.5) have same meaning as mentioned earlier.

$$\begin{aligned} perfn(1) = cL_F + T_{eq}\cos(\psi - i) - \{(W + Q_T - F_v)\sin\psi + F_h\cos\psi\} \\ + \left[(W + Q_T - F_v)\cos\psi + T_{eq}\sin(\psi - i) - F_h\sin\psi\right]\tan\phi = 0 \end{aligned} \tag{26.5}$$

Table 26.2 Statistical properties of random variables (i.e., in-situ soil parameters)

Parameter	Probability distribution	Mean value μ	[#]Coefficient of variation *COV* %		
			Minimum	Average	Maximum
Cohesion c	Lognormal	5 kPa	10	20	30
Angle of internal friction φ	Lognormal	30^0	02	06	10
Unit weight γ	Lognormal	16 kN/m^3	03	05	07
[#]—Phoon and Kulhawy [5], Duncan [6]					

Computational Global Stability Analysis

For the typical soil nail wall considered in the study, numerical simulations are performed using a commercially available finite element-based computational tool Plaxis 2D [15]. Global stability is assessed by determining factors of safety under static, pseudo-static, and dynamic conditions. Figure 26.3 shows the simulated model of the soil nail wall.

Plaxis uses strength reduction technique [22] for the computation of factor of safety. Strength reduction technique has the advantage that the critical failure mechanism is automatically identified. A plane strain state of stress using 15–node triangular elements with medium mesh density is assumed for numerical simulations. Soil nails and wall facing are simulated using plate elements behaving as linear elastic materials, and interfaces are considered rigid. The in-situ soil stress–strain behavior is simulated using Mohr–Coulomb material model. For dynamic analysis (i.e., time-history analysis), shear wave (V_S) and compression wave (Vp) velocities computed using elastic properties of soil E_S and μ are given as additional input parameters. The earthquake is modeled by imposing prescribed displacement at the bottom boundary and inputting the earthquake data corresponding to the time-history shown in the Fig. 26.2 as dynamic multiplier.

Further, simulation of construction stages is also performed. Soil nail wall is constructed in four stages represented as E1, E2, E3, and E4 in the Fig. 26.3. In each construction stage, installation of soil nails and facing elements is done after simulating an in-situ soil excavation of 2 m depth. For both static and dynamic analyses, standard simulation procedures with reference to the software manual [15] and details given in Singh and Sivakumar Babu [23] specifically on 2D numerical simulations of soil nails walls using Plaxis 2D software are followed.
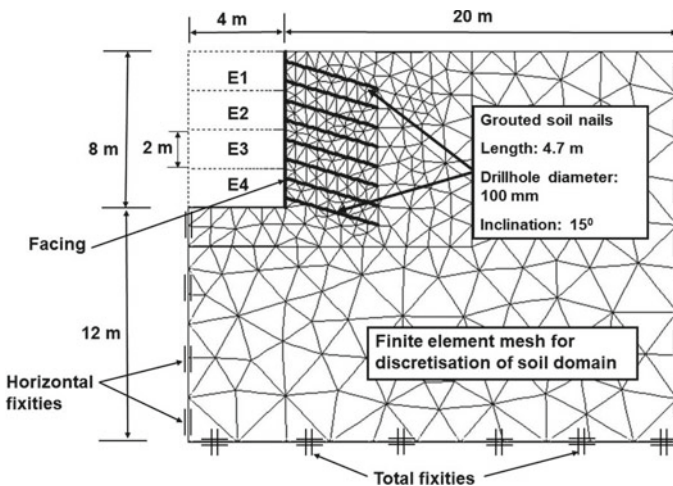

Fig. 26.3 Simulated model of soil nail wall

Results and Discussion

For the typical soil nail wall considered in the study, Plaxis is used for the numerical simulations. Further, using the deterministic expression given by Eq. (26.2), factor of safety values for global stability of the soil nail wall considered in the study are obtained as 1.81 and 1.65 for static and pseudo-static (for $k_h = 0.106$ and $k_v = 0.0$) conditions, respectively. Since these values of factor of safety are much more than the minimum desirable, the soil nail wall is safe against global failure. However, it is to be noted that these factors of safety values are computed corresponding to the mean values of in-situ soil parameters (i.e., cohesion, friction angle, and unit weight) given in Table 26.2. These mean values presume that both the resisting and driving components of the Eq. (26.1) have a probability of occurrence equal to unity, i.e., no uncertainty is involved in their determination. Thus, assessment of global stability merely based on deterministic approach is subjective and depends on the failure definition and the representative material parameters adopted. Also, the deterministic approach fails to provide any information about the associated probability of the failure.

To overcome the above-mentioned limitations of the deterministic approach, reliability-based evaluation of the global stability of the soil nail walls is expected to provide a better insight into the stability assessment. As stated earlier, the reliability indices are determined by Hasofer-Lind method using Eqs. (26.4) and (26.5), considering in-situ soil parameters (i.e., cohesion, friction angle, and unit weight) as uncorrelated lognormal random variables. According to Phoon [24], a reliability index β value equal to 3.0 signifies "*above average*" stability of the geotechnical structures, and the corresponding probability of failure P_f is approximately of the order of 1×10^{-3}. For high stability of geotechnical structures, minimum β is equal to 5.0 with $P_f \approx 3 \times 10^{-7}$.

Hasofer-Lind reliability index values for global stability β_{GL} were computed for both static and pseudo-static conditions. Further, to study the influence of uncertainty involved in determination of a given soil parameter, coefficient of variation (*COV*) of one parameter is varied at a time from its minimum to the maximum *COV* values mentioned in Table 26.2 and keeping *COVs* of other two parameters constant at their respective average values. Figure 26.4a–c shows variation in the reliability indices for global stability determined by considering the influence of uncertainty in the determination of in-situ soil parameters (i.e., c, φ, and γ). From Fig. 26.4a–c, it is evident that the uncertainty in the determination of in-situ soil friction angle has significant influence on the stability of soil nail wall. The trend is then followed by the unit weight and in-situ soil cohesion, respectively. Another observation from Fig. 26.4a–c is that for the soil nail wall under consideration, reliability index for global stability is more than 5.0 both in static as well as pseudo-static conditions. Thus, it is highly stable against global failure with probability of failure as low as 3×10^{-7}.

From the above discussion, it is apparent that reliability-based analysis provided much better insight into the global stability of soil nail wall in comparison to the
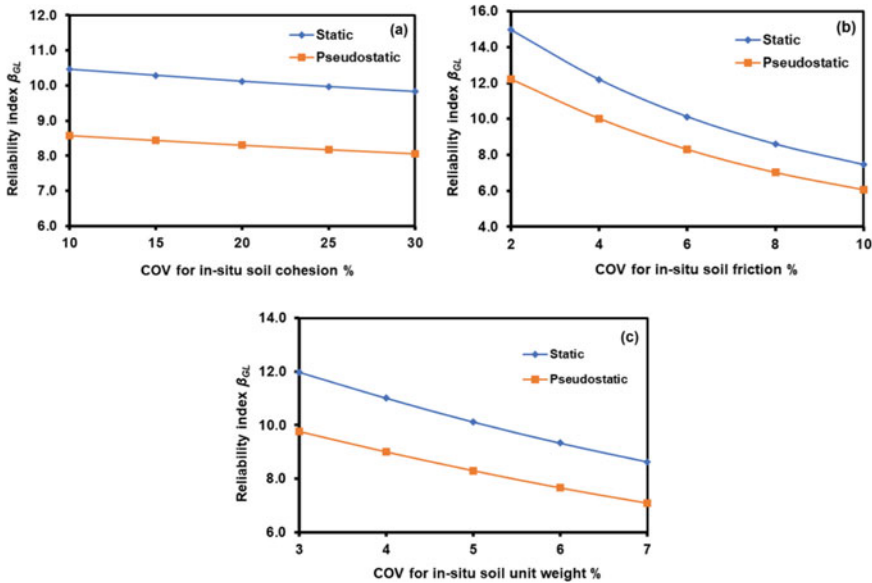
Fig. 26.4 Variation in reliability indices for global stability due the uncertainty in the determination of in-situ soil parameters: **a** cohesion, c, **b** friction angle, φ, **c** unit weight, γ

deterministic analysis. But, as stated earlier, factors such as composite structural behavior, complex soil–structure interaction, construction stages, 3D state of stresses, etc. greatly influences the long-term global stability of a soil nail wall. Both the above discussed deterministic and reliability-based approaches fail to address these aspects due to the complexity involved in their analytical modeling. Thus, for a holistic analysis of global stability of soil nail walls, computational modeling is an inevitable choice. Accordingly, factors of safety for global stability of the soil nail wall were computed using numerical simulations [15] for static, pseudo-static, and time-history (dynamic) analyses at its various construction stages E1, E2, E3, and E4. Table 26.3 summarizes the construction stage-wise factors of safety for global stability computed using numerical simulations. Construction stage is expressed as percentage of height of wall constructed upto the given excavation lift (in present case, each excavation lift is of 2 m) with respect to the full height of wall, i.e., 8 m.

From Table 26.3, it is evident that for 100% construction stage, i.e., fully constructed 8 m high wall, factors of safety are more than the minimum desirable factors of safety in static (i.e., 1.35–1.50) and seismic (i.e., 1.10) conditions, therefore, the given soil nail wall is stable against global failure. It is can also be noted from Table 26.3 that factors of safety against global stability have shown decreasing trend with construction stage. Further, Table 26.3 shows that the factor of safety value for dynamic analysis using time-history data for any given construction stage is relatively higher than the corresponding value using pseudo-static analysis. This observation may be attributed to the fact that in pseudo-static analysis seismic inertia forces are

Table 26.3 Summary of globality stability analyses using numerical simulations

Construction stage %	Legend (see Fig. 26.3)	Factor of safety, FS_G		
		Static analysis	Pseudo-static analysis	Time-history (dynamic) analysis
25	E1	2.40	1.80	1.90
50	E2	1.95	1.56	1.68
75	E3	1.75	1.42	1.55
100	E4	1.55	1.28	1.35

Table 26.4 Global stability assessment using different approaches

Analysis type	Deterministic approach	Reliability approach			Computational approach
		At minimum COVs	At average COVs	At maximum COVs	
Static	$FS_G = 1.81$	$\beta_{GL} = 21.97$	$\beta_{GL} = 10.12$	$\beta_{GL} = 6.52$	$FS_G = 1.55$
Pseudo-static	$FS_G = 1.65$	$\beta_{GL} = 18.04$	$\beta_{GL} = 8.30$	$\beta_{GL} = 5.33$	$FS_G = 1.28$
Time-history	–	–	–	–	$FS_G = 1.35$

Note All analyses performed using the mean values of soil parameters given in Table 26.2

considered to be continuously applied in the critical direction of loading, whereas in time-history analyses direction of loading keep changing with time resulting in both critical and non-critical loading combinations.

Table 26.4 presents a summary of global stability assessment of the soil nail wall of 8 m vertical height considered in the present study using different approaches, namely, deterministic, reliability based, and computational simulations.

From Table 26.4, it can be observed that for the same soil nail wall, global stability can be assessed and quantified differently depending upon the approach adopted for analysis. The factor of safety values obtained using computational approach are relatively less than the corresponding values using deterministic approach. Owing to the merits of computational analysis over conventional deterministic approach, global stability assessment using computational simulation can be considered as more realistic and accurate. Further, only a computational analysis can facilitate simulation of actual time-history data for seismic loading, which is certainly better than pseudo-static approach. Table 26.4 also highlights the importance of accurate determination of the representative mean soil parameters to be used for global stability analysis. It can be seen from Table 26.4 that the reliability indices corresponding to minimum *COVs* values are much higher than those corresponding to the maximum *COVs*. For example, for static analysis $\beta_{GL} = 21.97$ for the more accurate determination of soil parameters (i.e., minimum *COVs*) and $\beta_{GL} = 6.52$ for the less accurate determination of soil parameters (i.e., maximum *COVs*). As stated earlier, β_{GL} is directly linked to the probability of failure which in turn is a function of construction cost and anticipated risk.

Concluding Remarks

The present study highlighted the significance of multi-approach global stability analyses for soil nail walls. For illustration, a soil nail wall of vertical height 8 m was analyzed for global stability using conventional deterministic approach, reliability-based approach, and computational approach using a finite element-based software. Based on the results and discussions presented in the study, it can be concluded that the global stability analysis using computational approach is more realistic, and uncertainty involved in the determination of representative soil parameters should be addressed by the reliability-based approach. Therefore, it is recommended that for a more holistic global stability analyses, computational approach shall be invariably coupled with the reliability approach. Deterministic methods shall only be used for a preliminary study. Further, it is also recommended that time-history (dynamic) analyses shall be preferred over pseudo-static approach for studying the seismic stability of the soil nail wall.

References

1. Murthy BRS, Sivakumar Babu GL, Srinivas A (2002) Analysis of prototype soil nailed retaining wall. Ground Improvement 6(3):129–136
2. Sivakumar Babu GL, Murthy BRS, Srinivas A (2002) Analysis of construction factors influencing the behavior of soil nailed earth retaining walls. Ground Improvement 6(3):37–143
3. Sivakumar Babu GL, Rao RS, Dasaka SM (2007) Stabilisation of vertical cut supporting a retaining wall using soil nailing: a case study. Ground Improvement 11(3):157–162
4. FHWA0-IF-03–017 (2003) Geotechnical engineering circular no. 7 soil nail walls. Federal Highway Administration (FHWA), Washington D.C.
5. Phoon KK, Kulhawy FH (1999) Characterization of geotechnical variability. Can Geotech J 36(4):612–624
6. Duncan JM (2000) Factors of safety and reliability in geotechnical engineering. J Geotech Geo-Environ Eng 126(4):307–316
7. Felio GY, Vucetic M, Hudson M, Barar O, Chapman R (1990) Performance of soil nailed walls during the October 17, 1989 Loma Prieta earthquake. In: Proceedings of the 43rd Canadian geotechnical conference, Quebec, pp. 165–173
8. Vucetic M, Tufenkjian M, Doroudian M (1993) Dynamic centrifuge testing of soil-nailed excavations. ASTM Geotech Testing J 16(2):172–187
9. Tatsuoka F, Koseki J, Tateyama M (1997) Performance of reinforced soil structures during the 1995 Hyogo-ken Nanbu earthquake. In: Proceedings of the international symposium on earth reinforcement (IS Kyushu '96), Balkema, pp 973–1008
10. Tufenkjian MR, Vucetic M (2000) Dynamic failure mechanism of soil-nailed excavation models in centrifuge. J Geotech Geo-Environ Eng 126(3):227–235
11. Sivakumar Babu GL, Singh VP (2008) Numerical analysis of performance of soil nail walls in seismic conditions. ISET J Earthq Technol 45(1–2):31–40
12. Mokhtari M, Barkhordari K, Karafshani SA (2020) A comparative study of the seismic response of soil-nailed walls under the effect of near-fault and far-fault ground motions. J Eng Geol 13(5):121–146
13. Muthukumar S, Kolathayar S, Valli A, Sathyan D (2020) Pseudostatic analysis of soil nailed vertical wall for composite failure. Geomech Geoeng Int J. https://doi.org/10.1080/17486025.2020.1827163

14. Kramer SL (2003) Geotechnical earthquake engineering, 1st edn. Pearson Education, India
15. Plaxis: User manual, Plaxis bv, Bentley Systems Inc., The Netherlands (2020)
16. Hasofer AM, Lind NC (1974) Exact and invariant second moment code format. J Eng Mech 100(1):111–121
17. Sheahan TC, Ho CL (2003) Simplified trial wedge method for soil nailed walls analysis. J Geotech Geo-Environ Eng 129(2):117–124
18. Sivakumar Babu GL, Singh VP (2009) Reliability analysis of soil nail walls. Georisk: Assess Manage Risk Eng Syst Geohazards 3(1):44–54
19. Shrikhande M (2201) Atlas of Indian strong motion records. Department of Earthquake Engineering, Indian Institute of Technology, Roorkee
20. Low BK, Tang WH (1997) Efficient reliability evaluation using spreadsheet. J Eng Mech 123(7):749–752
21. Low BK (2005) Reliability-based design applied to retaining walls. Geotechnique 55(1):63–75
22. Matsui T, San KC (1992) Finite element slope stability analysis by shear strength reduction technique. Soils Found 32(1):59–70
23. Singh VP, Sivakumar Babu GL (2010) 2D numerical simulations of soil nail walls. Geotech Geol Eng 28(4):299–309
24. Phoon KK (2004) Towards reliability-based design for geotechnical engineering. Special Lecture for Korean Geotechnical Society, Seoul, pp 1–23